

# Estimation of the Wind Wave Spectra with Centimeters-to-Meter Lengths by the Sea Surface Images

V. V. Bakhanov<sup>1</sup>, A. A. Demakova<sup>1</sup>, A. E. Korinenko<sup>2</sup>,  
M. S. Ryabkova<sup>1</sup>, V. I. Titov<sup>1,\*</sup>

<sup>1</sup>*Institute of Applied Physics, Russian Academy of Sciences, Nizhny Novgorod, Russian Federation*

<sup>2</sup>*Marine Hydrophysical Institute, Russian Academy of Sciences, Sevastopol, Russian Federation*

\*e-mail: titov@hydro.appl.sci-nnov.ru

The method of investigating the sea wave spectra based on spectral processing of the sea surface images made at the diffused sky light is considered. The mechanisms of the sea surface image formation under the oblique viewing are discussed. It is shown that within the framework of a two-dimensional wave model and when the surface is illuminated by a clear sky, the sea surface image spectrum is proportional to that of the wave slopes' spectrum. Described is the developed in the Institute of Applied Physics, RAS optical incoherent light spectrum analyzer permitting to record two-dimensional spectra of the sea surface images in the real time mode. The spectrum analyzer has a wide dynamic range (up to 40–50 dB). The time required to record one two-dimensional spectrum is 1 sec. When the spectrum analyzer is set up at an oceanography platform or a ship bow, the device can record the wave spectra ranging from 1 meter to several centimeters depending on the height above the sea level and the viewing angle. The method for reconstructing the wave spectrum absolute values using the test object spectrum is represented. Preliminary results of the wave spectra measurements carried out by the optical method (under different wind speeds) from the stationary oceanographic platform in Katsiveli and from a moving vessel are given. The drawn conclusion testifies to conformity of the obtained wave spectra to the available empiric information on the spectra within the wind wave range under consideration. The obtained wave energy angular distributions and the spectra features observed in the slicks are discussed. To study the features of wave spectrum dynamics, developed is the method for imaging the current two-dimensional wave spectra with high resolution of spatial frequency and wave direction.

Time dependence of the wave angles' current spectra is represented as the horizontal bands; each of them corresponds to a certain direction of the wave propagation. At that the vertical direction in each band corresponds to the spatial frequency of the wave varying from short to long waves. The brightness of the images is proportional to the slope spectrum in the conventional color scale.

**Keywords:** sea surface, optics, surface image, surface brightness, processing of images, remote sensing, spectral analysis, wave spectrum, wind waves.

**For citation:** Bakhanov, V.V., Demakova, A.A., Korinenko, A.E., Ryabkova, M.S. and Titov, V.I., 2018. Estimation of the Wind Wave Spectra with Centimeters-to-Meter Lengths by the Sea Surface Images. *Physical Oceanography*, [e-journal] 25(3), pp. 177-190. doi:10.22449/1573-160X-2018-3-177-190

**DOI:** 10.22449/1573-160X-2018-3-177-190

© 2018, V. V. Bakhanov, A. A. Demakova, A. E. Korinenko, M. S. Ryabkova, V. I. Titov

© Physical Oceanography

## Introduction

The problem of remote diagnostics of sea waves has recently received much attention. In situ measurements of wind wave spectra have scientific and practical value. Nevertheless, there is still no sufficiently complete data on the short-wave spectrum directivity, on the frequency spectrum of short waves and on the transformation of wave spectra under effect of subsurface processes, as well as the ocean

surface pollution. Such information is necessary for the development of optical and radar (R) satellite methods for the ocean sensing.

There are the works [1–6], in which modern models of surface wave spectra used for solving remote sensing problems are discussed, an overview of popular spectral models and examples of solving the problems of reconstructing the sea surface characteristics from radar sounding data is given.

There are different ways of wave spectra measuring, including the ones using an array of string wave-recording gauges, but wave measurements do not have sufficient resolution for short-wave spectra recording. In [6, 7] the stereo images of sea waves obtained from the oceanographic platform are used to determine the spectra of short-scale wind waves. A semi-empirical spectrum model based on stereo-photography is also given in [6].

Spectral analysis of the sea surface images is, apparently, the only method for measuring two-dimensional wave spectra in the wide range of surface wave lengths from both the oceanographic platform and the moving carrier (ships, helicopters). Classic works on this subject [8] use a linear model of surface brightness dependence on the wave slopes when the surface is illuminated by the clear sky (or overcast sky) outside the zone of sun glints. In this case the spectrum of the sea surface image will be proportional to the one of the wave slopes. The image of the surface is recorded using a camera, TV-camera or a scanning optical-mechanical device with the following spectral processing. The Institute of Applied Physics (IAP RAS) developed the methods for diagnosing the wave spectra from optical images of the sea surface and designed a number of incoherent optical analyzers of the sea surface image spectrum in real time, which are used within a ship complex to study the wave transformation in the surface slicks, in the field of internal waves, above the inhomogeneities of the underwater relief (for example, sea mounts), in the zones of algal blooms, etc. [8–12].

### The models of wave visibility

The model of the surface brightness  $I$  dependence on the wave slopes when illuminated by clear sky or uniformly overcast sky in the first approximation uses a linear dependence [13]

$$I(\mathbf{q}) = I_0 + \mathbf{q}\nabla I. \quad (1)$$

Brightness fluctuations are proportional to the product of the surface brightness gradient  $\nabla I = (\partial I/\partial q_x, \partial I/\partial q_y)$  by a vector of wave slopes  $\mathbf{q} = (\partial z/\partial x, \partial z/\partial y)$  where  $z(x, y)$  are the wave elevations;  $I_0$  is a mean brightness of a sea surface.

On the sea surface the highest optical contrast will have the waves propagating in the direction of the brightness gradient, and the waves propagating perpendicular to the brightness gradient will not be visible. The wave spectrum within the framework of the linear model can be estimated from the spectrum of the sea surface image  $G_I$ :

$$G_I(\mathbf{k}) = (\mathbf{k}\nabla I)^2 G(\mathbf{k}) = (\mathbf{k}^2 \nabla I^2 \cos^2 \alpha) G(\mathbf{k}), \quad (2)$$

where  $G(\mathbf{k})$  is a spectrum of the sea surface elevations;  $\mathbf{k}$  is a wave vector;  $\alpha$  – is an angle between the surface brightness gradient and the direction of the surface wave propagation. Expression  $(\mathbf{k}\nabla I/|\nabla I|)^2 G(\mathbf{k})$  is called a spectrum of wave slopes in the direction of surface brightness gradient  $\nabla I/|\nabla I|$ . The spectrum of a sea surface image will be equal to zero for the waves with a propagation direction perpendicular to the brightness gradient.

Sea surface brightness is equal to the product of the sky brightness by Fresnel light reflection coefficient, and the visible wave contrasts will be determined by both the angular dependence of the sky brightness for the mirror section of the sky and the dependence of Fresnel coefficient on the local light incidence angle. When performing the observations in the counter-sun directions under the sliding angles, the surface brightness gradient will be oriented in the viewing direction.

Further development of this model is connected with the consideration of the square term in the surface brightness expansion by levels of wave slopes, which made it possible to assess the accuracy of the wave spectrum estimate by the formula (2) [13].

New approach to the wave spectrum estimation is associated with the use of a two-scale wave model [14]. Sea roughness is presented as an ensemble of non-interacting free waves. The surface elevations are expressed as the sum of the elevations of long and short waves corresponding to the wave spectrum partitioning into two adjacent regions of small and large wave numbers, respectively:

$$z(x, y) = z_l + z_s,$$

and a vector of slopes is expressed as a sum of two vectors: gradients of long waves  $\mathbf{q}_l = (\partial z_l / \partial x, \partial z_l / \partial y)$  and short waves  $\mathbf{q}_s = (\partial z_s / \partial x, \partial z_s / \partial y)$ :

$$\mathbf{q} = \mathbf{q}_l + \mathbf{q}_s. \quad (3)$$

We expand the surface brightness in a series by the levels of short wave slopes  $\mathbf{q}_s$  in a local point at a long wave  $\mathbf{q}_l$  confining ourselves to a second-order term of smallness. We consider the case when the surface brightness  $I$  depend on the slopes of short waves in one direction  $q_1(r, t) = q_{l1} + q_{s1}$ :

$$I(q_1) = I(q_{l1}) + I'(q_{l1})q_{s1} + \frac{1}{2}I''(q_{l1})q_{s1}^2, \quad (4)$$

where  $I'(q_{l1}) = \partial I / \partial q_1$  and  $I''(q_{l1}) = \partial^2 I / \partial q_1^2$  are the surface brightness derivatives by  $q_1$ .

For instance, when observing from a vessel or a sea platform under the sliding angles at a clear sky (when the sun is behind) or at an overcast sky, the sea surface brightness will be a function of wave slopes in the direction of viewing.

Then from the formulas (2) and (4) such expression for the image spectrum will follow:

$$G_I(\mathbf{k}) = I'^2 \left( 1 + \frac{I''^2}{I'^2} \langle q_{l1}^2 \rangle \right) k_1^2 G(\mathbf{k}). \quad (5)$$

Long waves cause the contrast modulation of the short waves under analysis and this leads to the change of coefficient ahead of the spectrum of short waves. It follows from the formula (5) that relative measurements of wave spectrum (spectral contrasts, frequency and angular spectrum characteristics) have higher accuracy than the absolute measurements.

#### **Description of two-dimensional optical spectrum analyzer (TOSA).**

In IAP RAS an incoherent two-dimensional optical spectrum analyzer for the sea surface image spectral analysis in real-time regime without intermediate registration, which uses a principle of image modulation by a standard with harmonic distribution of transparency coefficient [15], is developed. A cycle of measuring the two-dimensional spectrum of the image by the TOSA analyzer takes 1 second. During this time, a spectrum of 140 spatial frequencies for 32 wave directions in 120° angular sector ( $\pm 60^\circ$  from the TOSA viewing direction) with an angular resolution of approximately  $3.7^\circ$  is registered. The range of the spectrum spatial frequencies depends on the observation geometry and the focal distance of the object lens.

In order to obtain two-dimensional spectra, the surface image modulation using a rotating reference disc with a harmonic distribution of the transparency coefficient (the spatial frequency of the transparency coefficient varies along the perimeter of the disk) and an additional revolution of the water surface image with a prism (the so-called Pekhan prism is applied) are used. The prism performs stepwise rotational movements forward and backwards in a certain angular range. Rotation of the standard reference disc and the one of the prism are synchronized in such a way that with one revolution of the disk the prism rotates by one small step. It can be several dozen of such steps or directions of the analyzed waves depending on the required size of two-dimensional spectrum. A modulated image is collected by a lens to the photo detector.

The analyzer also generates a signal proportional to the sea surface brightness. For this purpose the constant component of the transparency coefficient standard is used. TOSA is supplemented with a scanning brightness gauge for recording the sea brightness  $I_0$  and the surface brightness gradient  $\nabla I$  of the (formula (1)) synchronously with the analyzer signals.

All the signals are recorded on the laptop hard disk through the input card. TOSA signal processing program, which includes the formation of estimation of the sea surface image energy spectrum by raising the TOSA signal to the square, normalizing the surface integral brightness by the square and by the normalized energy spectrum of the standard, bringing the spectrum to the coordinates at the sea surface, averaging a certain number of spectra for obtaining a statistically-provided estimate of the wind wave spectrum, is developed.

Instantaneous Fourier transformation allows one to increase the dynamic range and avoid image blurring caused by ship motion, which is an advantage of the developed device for optical spectral processing of a rough surface image over similar devices with TV cameras. Due to this, it is possible to record the spectra of arbitrarily short waves, which the observation geometry can only allow, along the vessel path.

## The development of a physical algorithm for reconstructing the absolute values of the wave slope spectrum from the sea surface image spectrum

The problem is solved in two stages.

### 1. Calibration of the optical spectrum analyzer.

At this stage the frequency-contrast characteristic (FCC) of spectrum analyzer is determined. Usually, test objects of striped type with a narrow spatial spectrum are used for this purpose. In our case, a test object with an isotropic wide spectrum within the TOSA frequency range was selected. Such test object not only provided a calibration of FCC but also a construction of an algorithm for reconstructing the wave spectrum absolute values. This test object is represented by random white dots against black background [16] and the centers of the dots are distributed over the area according to Poisson law: the coordinates of dot centers are uniformly distributed (Fig. 1).

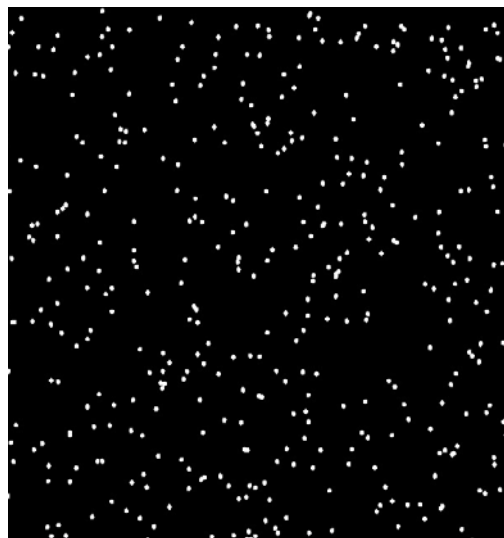


**Fig. 1.** Fragment of the test-object for the TOSA calibration

It is assumed that the test object points are rare, i.e. they do not overlap each other and the diameter of the points in the plane of the TOSA image (in the plane of the standard) is much smaller (by an order of magnitude) than the minimum period of the transmission coefficient of the standard.

### 2. Reconstruction of wave spectrum absolute values.

TOSA signals are registered in volts.

Average signal of the TOSA optical spectrum analyzer after a computer processing, described in the previous section, will be proportional to the energy spectrum of the sea surface brightness distribution:

$$U = A^2 \left| \int I(\mathbf{r}, t) \exp(\mathbf{k}\mathbf{r}) d\mathbf{r} \right|^2 = A^2 (2\pi)^2 S \tilde{G}_I(\mathbf{k}), \quad (6)$$

where  $A$  is a proportionality coefficient;  $\tilde{G}_I(\mathbf{k})$  is an estimation of energy spectrum of the sea surface brightness distribution  $I$ :

$$\tilde{G}_I(\mathbf{k}) = \frac{1}{(2\pi)^2 S} \left| \int I(\mathbf{r}, t) \exp(\mathbf{k}\mathbf{r}) d\mathbf{r} \right|^2,$$

where  $S$  is an area of a field of view. Integral is taken from the TOSA field of view. The average of an estimate is equal to the image energy spectrum.

A signal proportional to the sea surface integral brightness along the field of view is also recorded (formula (1)):

$$P = K \int I(\mathbf{r}, t) d\mathbf{r} = KSI_0,$$

where  $K$  is a proportionality coefficient.

The same expressions can be written down for the test object brightness distribution.

Let us form a relation

$$\frac{UP_t^2}{U_t P^2} = \frac{(2\pi)^2 G_t(\mathbf{k})}{SI_0^2} \frac{A^2 K_t^2}{A_t^2 K^2} \frac{(2\pi)^2 G_t(\mathbf{k})}{S_t I_t^2}, \quad (7)$$

Where the subscript  $t$  is related to the test object. This expression contains the desired relation

$$\frac{G_t(\mathbf{k})}{I_0^2} = \left( \mathbf{k} \frac{\nabla I}{I_0} \right)^2 G(\mathbf{k}), \quad (8)$$

Where dimensionless relation  $\frac{\nabla I}{I_0}$  can be calculated according to the models of the

sky brightness distribution, angular distribution of the sky brightness measured in the experiment (at sliding viewing angles the light polarization should be considered) [18] or it can be measured with a scanning brightness gauge described above. Theoretical estimates and in situ measurements of brightness gradient relation to the mean sea brightness for the clear sky and unpolarized light gave the values in modulus within 4–6 range. For the estimation of values of the recorded spectra in

Fig. 3–7 the value equal to 4 of the relation  $\left| \frac{\nabla I}{I_0} \right|$  was chosen.

The same relation for the test object  $\frac{(2\pi)^2 G_t(\mathbf{k})}{S_t I_t^2}$  is calculated. This relation

can be estimated as  $\frac{1}{N_t}$ , where  $N_t$  is a number of test dots in the TOSA field of view. There are  $N_t = 3 \cdot 10^3$  dots in the experiment with test object.

The relations of  $\frac{A}{A_t}$  and  $\frac{K}{K_t}$  coefficients are calculated through the relations of gain coefficients in the channels of spectrum and brightness. It should be pointed

out that this technique provides a consideration of optical path light transmission coefficients, including the value of the lens diaphragm, which are automatically taken into account when forming the relations (7) for the sea and the test objects.

Thus, this technique (formula (7)) allows us to reconstruct the spectrum of wave slopes and, from the models described in the first section of the article, we can determine the wave elevation spectrum, while we only need to know the values of the brightness gain coefficients and spectra in field experiments and in the experiment with the test objects.

### Wave spectra measurements

Wave spectra recording with the TOSA was carried out on the oceanographic platform in Katsiveli from October 4 to October 10, 2016.

In Fig. 2 and 3 wind velocity and direction graphs for 06.10.2016 are given. Meteorological station of Marine Hydrophysical Institute of RAS was installed on the upper deck (17 m above the sea level). The arrows indicate the instants of time when the spectra listed below were recorded.

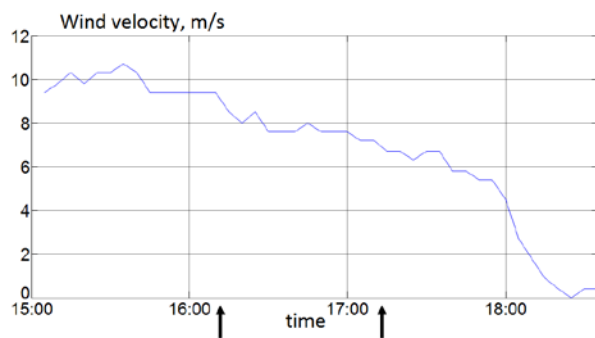


Fig. 2. Wind velocity, m/s, 06.10.2016

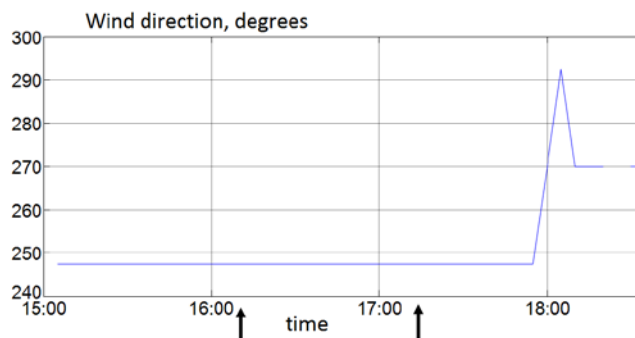
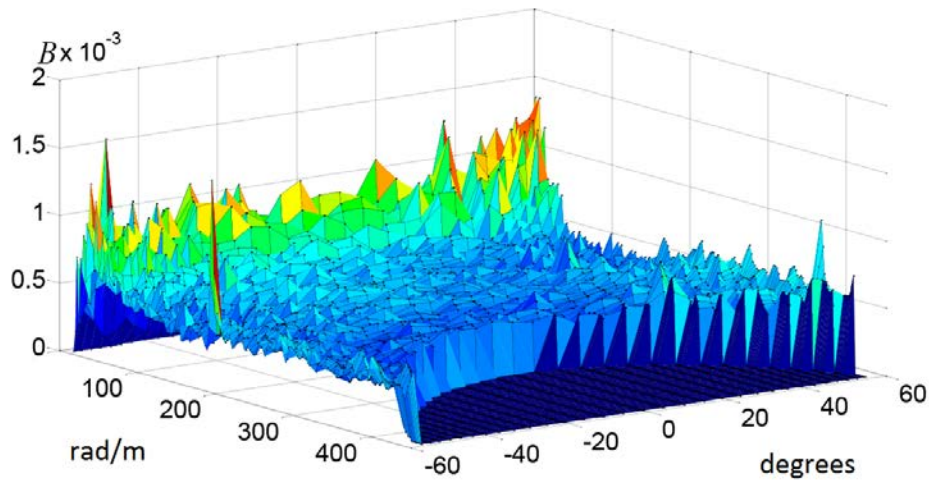


Fig. 3. Wind direction, 06.10.2016

Further we move on to Philips dimensionless spectrum of saturation [18]:  $B = k^4 G(\mathbf{k})$ . In Fig. 4 two-dimensional wave spectrum  $B$  in the coordinates, wave number on the sea surface in rad/m and an angle between wave propagation direction and TOSA viewing angle are represented. TOSA was installed on a lower bridge (4.5 m height above the sea level). Viewing is directed to the east along the

seaward part of the platform. A part of spectrum is absent (spectrum values are set to be equal to zero) which is determined by perspective image distortions at the oblique viewing. The spectrum is obtained by averaging 200 spectra in 200 s. The accompanying wind conditions are shown by the left arrow in Fig. 2 and 3.



**Fig. 4.** Two-dimensional spectrum of the waves  $B$  (Philips saturation spectrum [18]): wave number in rad/m is plotted on the left axis; wave direction in degrees relative to the TOSA viewing direction – on the right axis

O. M. Philips [18] forms so-called *omnidirectional spectra* (spectrum integrated over the wave directions  $\alpha$ ):

$$\chi(k) = \int_0^{2\pi} G(\mathbf{k}) k d\alpha = k^{-3} \int_0^{2\pi} B d\alpha = B_s k^{-3}$$

If for the estimation we assume that the spectrum is isotropic ( $B(\alpha) = \text{const}$ ), then for the short waves ( $k > 50$  rad/m or the wave length  $\lambda < 13$  cm)  $B_s = 2\pi B \approx 2,5 \cdot 10^{-3}$  which corresponds to the data of other authors [7].

In Fig. 5 angular spectra of the waves for this two-dimensional spectrum are shown. The notes indicate the wave length. Wind direction lies near the extreme angles of the spectrum: the spectra increase toward the extreme angles. Angular spectra demonstrate anisotropy: they increase toward the direction of the wind. The angular anisotropy of the spectra reduces with a wavelength decrease.



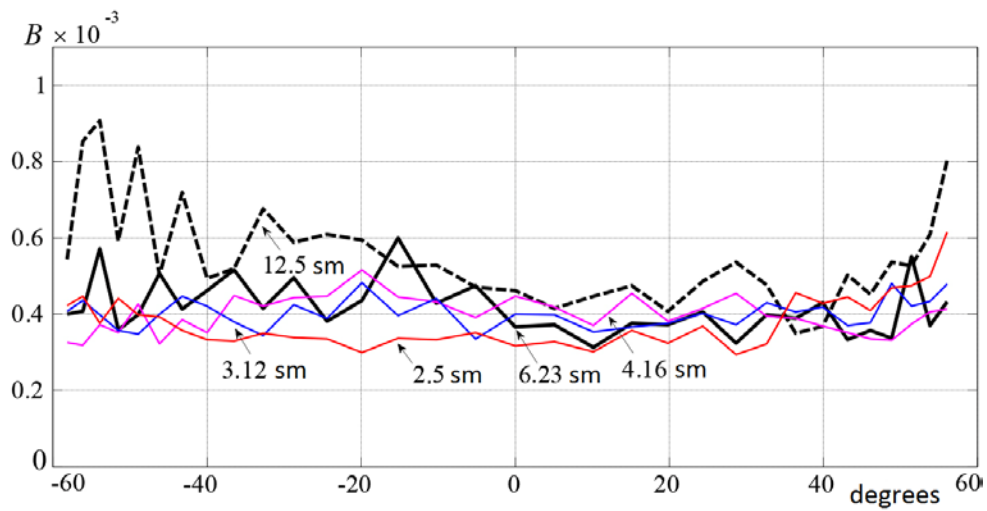


Fig. 5. Angle spectra of waves. The notes show the wave length  $\lambda = 2\pi/k$

The second spectrum (Fig. 6) was obtained by averaging 100 spectra in 100 s under conditions of non-stationary wind field when new wing gusts occurred from another direction (IAP RAS data). Corresponding wind conditions are shown by the right arrow in Fig. 2 and 3.

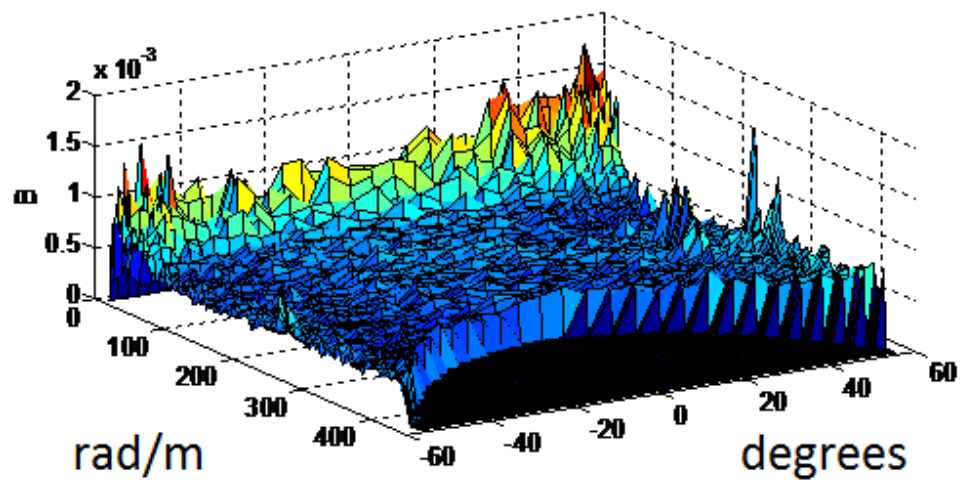


Fig. 6. Two-dimensional spectrum of the waves  $B$ : wave number in rad/m is plotted on the left axis; wave direction in degrees relative to the TOSA viewing direction – on the right axis

In Fig. 7 angular spectra of the waves for this two-dimensional spectrum are given. The notes show the wave height.

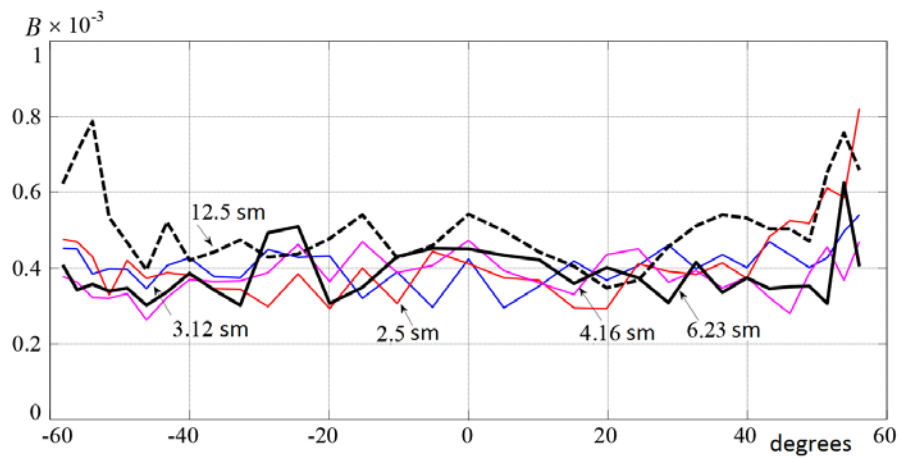


Fig. 7. Angle spectra of waves. The notes show the wave length  $\lambda = 2\pi/k$

In Fig. 8 two-dimensional wave spectrum  $B$  obtained on 07.10.2016 at 15:30 is represented. The wind was of the western direction and near the eastern corner of the platform where the TOSA was installed (at 14 m height above the sea level) a slick occurred. The outlines and boundaries of the slick randomly changed. In Fig. 8 the smoothing of the water surface (the spectrum decrease) for the waves with a wave number of about 20–25 rad/m and a propagation direction from 20 to 40 ° due to this slick can be seen. The spectrum was obtained by averaging 200 spectra in 200 s.

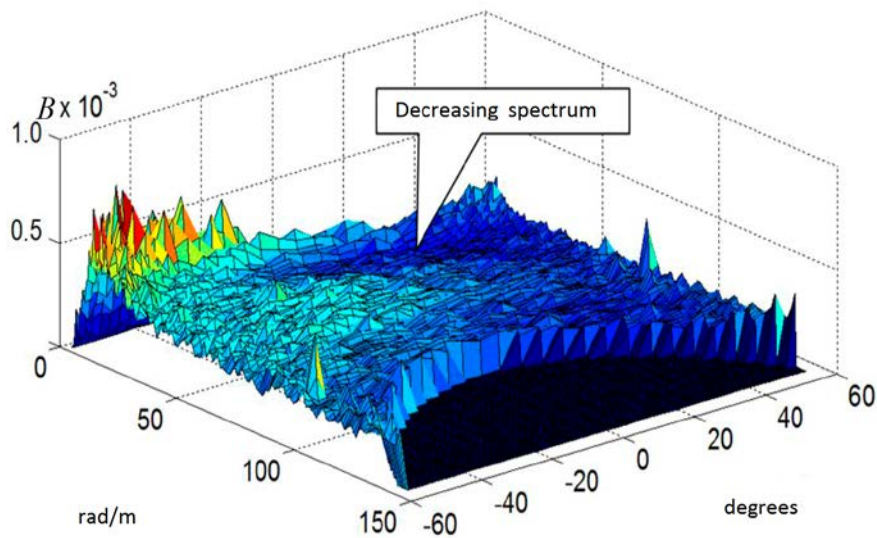


Fig. 8. Two-dimensional spectrum of the waves  $B$ : wave number in rad/m is plotted on the left axis; wave direction in degrees relative to the TOSA viewing direction – on the right axis

### The study of transformation of wave slope spectra in slicks

For studying the features of wave spectrum dynamics a program for representing the two-dimensional current TOSA spectra with a good resolution in terms of the spatial frequency and direction of the waves was developed.

Current spectra of wave slopes depending on the time are presented in the form of horizontal bands, each of which corresponds to a certain direction of wave propagation. The spatial frequency of the wave varies from short to long waves changing vertically within each strip. The brightness of the images will be proportional to the slope spectrum in the conventional color scale.

An example of slope spectra recordings in a calm day is given in Fig. 9. The TOSA analyzer was installed at a bow of a moving vessel. Calm zones were replaced by wave generation areas and slick stripes.

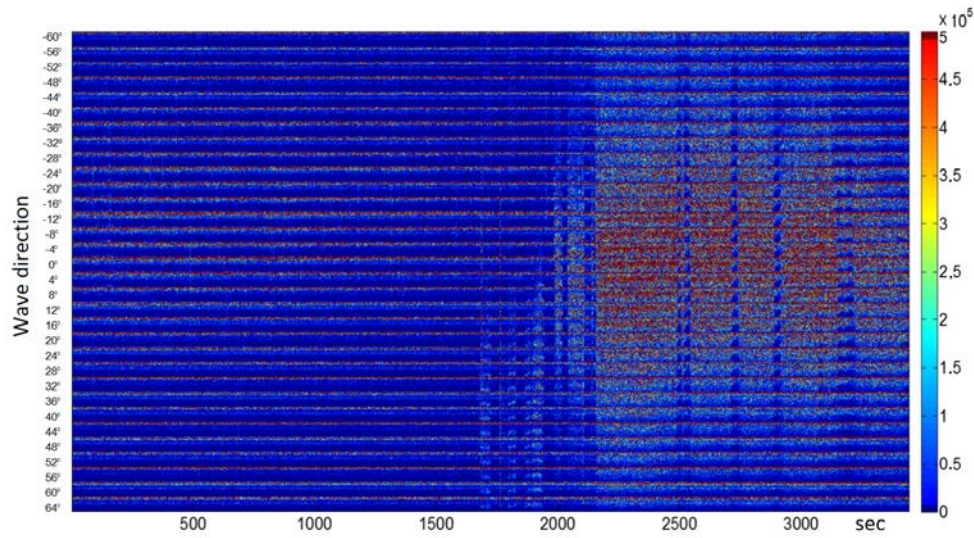


**Fig. 9.** Spectra of wave slopes: along the horizontal – time in seconds, along the vertical – the bands corresponding to 32 directions of wave propagation in approximately every 4° in a wave direction range  $\pm 60^\circ$  relative to the TOSA viewing direction (direction 0° corresponds to the TOSA viewing direction). The wave spatial frequency corresponding to the wavelengths from 70 to 3 cm is plotted (top-down mode, linear scale) along the vertical in the each band corresponding to a certain wave direction

As is obvious from Fig. 10, the spectra of developing waves are significantly anisotropic in spatial frequency with a maximum in the area of waves of 15–20 cm length.

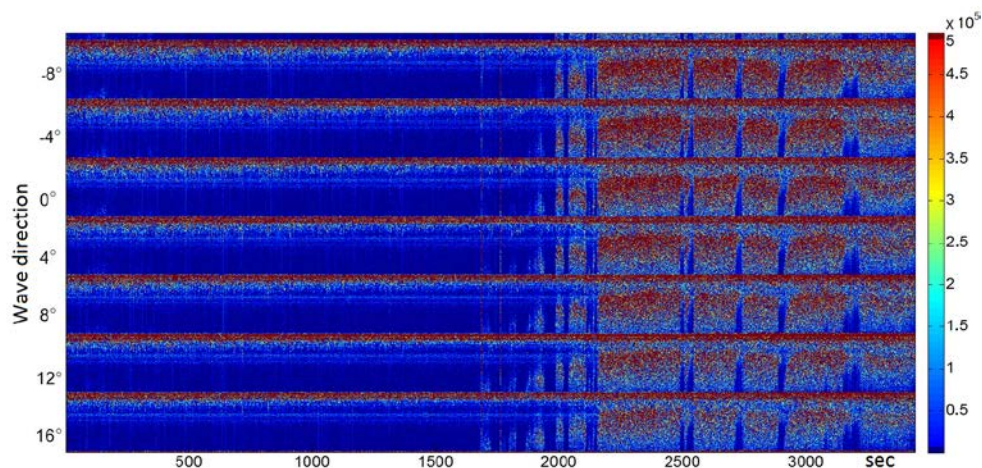


**Fig. 10.** Wave spectra for a few wave directions nearby the TOSA viewing direction

The developed method and equipment are unique and allow one to study two-dimensional wave spectra from a hydrophysical platform and from a moving vessel in real time, as is shown in this example.

#### REFERENCES

1. Elfouhaily, T., Chapron, B., Katsaros, A. and Vandemark, D., 1997. A Unified Directional Spectrum for Long and Short Wind-Driven Waves. *Journal of Geophysical Research*, [e-journal] 102(C7), pp. 15781-15796. doi:10.1029/97JC00467
2. Karaev, V.Yu. and Balandina, G.N., 2000. Modifitsirovannyi Spekr Volneniya i Distantionnoe Zondirovanie Okeana [A Modified Wave Spectrum and Remote Sensing of Ocean]. *Issledovanie Zemli iz Kosmosa*, (5), pp. 45-56 (in Russian).
3. Karaev, V., Kanevsky, M. and Meshkov, E., 2008. The Effect of Sea Surface Slicks on the Doppler Spectrum Width of a Backscattered Microwave Signal. *Sensors*, [e-journal] 8(6), pp. 3780-3801. doi:10.3390/s8063780
4. Ryabkova, M.S., Karaev, V.Yu., Panfilova, M.S. and Titchenko, Yu.A., 2017. Spektiry Poverkhnostnogo Volneniya dlya Zadach Distantionnogo Zondirovaniya: Obzor Populyarnykh Modeley i Obsuzhdenie Novoy Modeli [Surface Wave Spectra for Remote Sensing: Review of Popular Models and Discussion of New Model]. In: SRI, 2017. *XV Vserossiyskaya Otkrytaya Konferentsiya Sovremennye Problemy Distantionnogo Zondirovaniya Zemli iz Kosmosa* [15th Conf. Current Problems in Remote Sensing of the Earth from Space]. Book of Abstracts. Moscow: SRI, pp. 286 (in Russian).
5. Ryabkova, M.S., Karaev, V.Yu., Titchenko, Yu.A. and Meshkov, E.M., 2017. Experimental Study of the Microwave Radar Doppler Spectrum Backscattered from the Sea Surface at Low Incidence Angles. In: URSI GASS (The International Union of Radio Science General Assembly and Scientific Symposium), 2017. *XXXIIth General Assembly and Scientific Symposium of the International Union of Radio Science*, Montreal, QC, Canada, 19-26 Aug. 2017. IEEE, pp. 1-4. doi:10.23919/URSIGASS.2017.8105008
6. Yurovskaya, M.V., Dulov, V.A., Chapron, B. and Kudryavtsev, V.N., 2013. Directional Short Wind Wave Spectra Derived from the Sea Surface Photography. *Journal of Geophysical Research*, [e-journal] 118(9), pp. 1-15. doi:10.1002/jgrc.20296
7. Kosnik, M.V. and Dulov, V.A. Extraction of Short Wind Wave Spectra from Stereo Images of the Sea Surface. 2011. *Measurement Science and Technology*, [e-journal] 22(1), 015504. doi:10.1088/0957-0233/22/1/015504

8. Titov, V.I., Bakhanov, V.V., Zuiikova, E.M., Luchinin, A.G. and Troitzkaya, J.I., 2010. Issledovanie Dinamiki Dvumernykh Spektrov Morskogo Volneniya [Investigation of Dynamic of Two Dimensional Spectra of Sea Waves]. *Sovremennye Problemy Distantionnogo Zondirovaniya Zemli iz Kosmosa = Current Problems in Remote Sensing of the Earth from Space*, 7(1), pp. 273–285 (in Russian).
9. Titov, V.I., Zuiikova, E.M. and Luchinin, A.G., 2010. Issledovanie Prostranstvenno-Vremennykh Spektrov Korotkomasshtabnogo Volneniya Opticheskim Metodod [Investigation of Space and Temporal Spectra of Small-Scale Water Surface Waves by Optical Methods]. In: MHI, 2010. *Ekologicheskaya Bezopasnost' Pribrezhnoy i Shel'fovoy Zon i Kompleksnoe Ispol'zovanie Resursov Shel'fa* [Ecological Safety of Coastal and Shelf Zones and Comprehensive Use of Shelf Resources]. Sevastopol: MHI NANU. Iss.21, pp. 197-206 (in Russian).
10. Titov, V.I., Bakhanov, V., Ermakov, S., Kapustin, I., Luchinin, A., Sergievskaja, I. and Zuiikova, E., 2012. Development of Optical Remote Sensing Technique for Monitoring of Water Basins. In: SPIE, 2012. *Remote Sensing of the Ocean, Sea Ice, Coastal Waters, and Large Water Regions*. Bellingham, Washington, 19 October 2012. Bellingham: SPIE. Vol. 8532. doi:10.1117/12.974421
11. Titov, V., Bakhanov, V., Ermakov, S., Luchinin, A., Repina, I. and Sergievskaya, I., 2014. Remote Sensing Technique for Near-Surface Wind by Optical Images of Rough Water Surface. *International Journal of Remote Sensing*, 35(15), pp. 5946-5957. doi: 10.1080/01431161.2014.948223
12. Titov, V.I., Artamonov, A.Yu., Bakhanov, V.V., Ermakov, S.A., Luchinin, A.G., Repina, I.A. and Sergievskaja, I.A., 2014. Monitoring Sostoyaniya Poverkhnosti Morya po Prostranstvenno-Vremennym Opticheskim Izobrazheniyam [Monitoring of Sea Surface with Optical Technique]. *Issledovanie Zemli iz Kosmosa*, (5), pp. 3-14 (in Russian).
13. Chapman, R.D. and Irani, G.B., 1981. Errors in Estimating Slope Spectra from Wave Images. *Applied Optics*, [e-journal] 20(20), pp. 3645-3652. doi:10.1364/AO.20.003645
14. Bakhanov, V.V., Zuiikova, E.M., Kemarskaya, O.N. and Titov, V.I. 2006. Determining the Sea-Roughness Spectra from an Optical Image of the Sea Surface. *Radiophysics and Quantum Electronics*, [e-journal] 49(1), pp. 47-57. <https://doi.org/10.1007/s11141-006-0036-y>
15. Zuiikova, E.M., Titov, V.I. and Troitskaya, Yu.I., 2010. *Ustroystvo Opticheskoy Spektral'noy Obrabotki Izobrazheniya Sherokhovatoy Poverkhnosti* [Rough Surface Image Optical Spectral Processing Device]. Patent 2400705 Russian Federation, No. 2009103024. <http://www.freepatent.ru/images/patents/62/2400705/patent-2400705.pdf> (in Russian).
16. O'Neill, E.L., 1963. *Introduction to Statistical Optics*. New York: Addison-Wesley Publishing Co., Inc., 186 p.
17. Brunger, A.P. and Hooper, F.C., 1993. Anisotropic Sky Radiance Model Based on Narrow Field of View Measurements of Shortwave Radiance. *Solar Energy*, [e-journal] 51(1), pp. 53-64. doi:10.1016/0038-092X(93)90042-M
18. Phillips, O.M., 1977. *The Dynamics of the Upper Ocean*. Cambridge: University of Cambridge Press., 320 p.

*About the authors:*

**Victor V. Bakhanov** – the head of Laboratory of Hydrophysical and Acoustic Modeling, FRC Institute of Applied Physics of the Russian Academy of Sciences (46, Ulyanov str., Nizhny Novgorod, 603950, Russian Federation), Ph.D. (Phys.-Math.), ID: 6603623205, [bakh@hydro.appl.sci-nnov.ru](mailto:bakh@hydro.appl.sci-nnov.ru)

**Anastasia A. Demakova** – research assistant, post-graduate student, FRC Institute of Applied Physics of the Russian Academy of Sciences (46, Ulyanov str., Nizhny Novgorod, 603950, Russian Federation), [d6365@yandex.ru](mailto:d6365@yandex.ru)

**Aleksandr E. Kornienko** – research associate, FSBSI MHI (2, Kapitanskaya Str., Sevastopol, 299011, Russian Federation), Ph.D. (Phys.-Math.), Scopus Author ID: 23492523000, [korinenko.alex@gmail.com](mailto:korinenko.alex@gmail.com)

**Mariya S. Ryabkova** – research assistant, post-graduate student, FRC Institute of Applied Physics of the Russian Academy of Sciences (46, Ulyanov str., Nizhny Novgorod, 603950, Russian Federation), Scopus AuthorID: 57192586907; m.rjabkova@gmail.com

**Victor I. Titov** – senior research associate, FRC Institute of Applied Physics of the Russian Academy of Sciences (46, Ulyanov str., Nizhny Novgorod, 603950, Russian Federation), Ph.D. (Phys.-Math.), Scopus Author ID: 7201990965, titov@hydro.appl.sci-nnov.ru

*Contribution of the co-authors:*

**Victor V. Bakhanov** – scientific supervision, participation in discussions on the article materials

**Anastasia A. Demakova** – experimental research, experimental data processing, description of the results

**Aleksandr E. Kornienko** – development of methodology, experimental research, analysis and synthesis of the research results

**Mariya S. Ryabkova** – review of the literature on the research problem

**Victor I. Titov** – general scientific supervision of research, processing and description of research results, preparation of the article

*The authors have read and approved the final manuscript.*

*The authors declare that they have no conflict of interest.*